

Earth factories: Creation of the elements from nuclear transmutation in Earth's lower mantle

Cite as: AIP Advances 11, 105113 (2021); doi: 10.1063/5.0061584

Submitted: 28 June 2021 • Accepted: 25 August 2021 •

Published Online: 12 October 2021



Mikio Fukuhara,^{1,2,a)}  Alexander Yoshino,³  and Nobuhisa Fujima⁴ 

AFFILIATIONS

¹New Industry Creation Hatchery Centre, Tohoku University, Sendai 980-8579, Japan

²Research Organization for Nano and Life Innovation, Green Device Laboratory, Waseda University, Tokyo 162-0041, Japan

³Statistical and Computer Sciences, New College, University of Toronto, Toronto, Ontario M5S1C6, Canada

⁴Faculty of Engineering, Shizuoka University, Hamamatsu 432-8561, Japan

^{a)}Author to whom correspondence should be addressed: mikio.fukuhara.b2@tohoku.ac.jp

ABSTRACT

Stellar nucleosynthesis is a widely acknowledged theory for the formation of all elements in our universe; traditionally, we say that the highest mass stars transmuted lighter elements into heavier elements lighter than iron. Here, we propose that the formation of 25 elements with smaller atomic numbers than iron resulted from an endothermic nuclear transformation of two nuclei confined in the natural compound lattice core of the Earth's lower mantle at high temperatures and pressures. This process is accompanied by the generation of neutrinos and is influenced by excited electrons generated by stick-sliding during supercontinent evolution, mantle convection triggered by major asteroid collisions, and nuclear fusion in the Earth's core. Therefore, our study suggests that the Earth itself has been able to create lighter elements by nuclear transmutation.

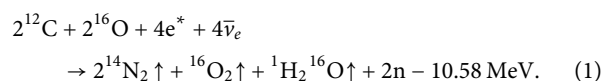
© 2021 Author(s). All article content, except where otherwise noted, is licensed under a Creative Commons Attribution (CC BY) license (<http://creativecommons.org/licenses/by/4.0/>). <https://doi.org/10.1063/5.0061584>

I. INTRODUCTION

The Big Bang theory¹ proposes that hydrogen, helium, and trace amounts of lithium were the only elements in existence when the universe first formed. In other words, Big Bang nucleosynthesis produced elements no heavier than lithium. Hotter and heavier stars then transmuted lighter elements (i.e., the first elements) into heavier elements (i.e., the secondary elements, some of which were generated by the CNO cycle²) up to and including iron through exothermic stellar nucleosynthesis in their cores. Because the fusion of iron nuclei does not create energy, high mass star cores must collapse, resulting in supernovae. When supernovae explode, many neutrons passing through the outer regions of the stars collide with the atoms of elements lighter than iron (number 26 in the periodic table), resulting in elements heavier than iron via neutron incorporation.³ This theory is the basis of convention for the formation of all elements in our universe. Regarding Earth formation, it is generally believed that the terrestrial planets have formed by accretion of solid materials that condensed from the solar nebula

~4.56 × 10⁹ years ago.⁴ As a result, whole-Earth geochemical models, which are primarily based on cosmochemical abundances, provide specific limits on the possible chemical composition of the Earth's deep interior.⁵

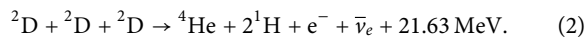
In disagreement with this theory, Fukuhara proposed a model for the formation of nitrogen, oxygen, and water using circumstantial evidence based on the history of the Earth's atmosphere. This hypothesis suggests that heavier elements result from an endothermic nuclear transformation of carbon and oxygen nuclei confined in the aragonite CaCO₃ lattice of the Earth's mantle or crust, which is enhanced by the attraction caused by high temperatures ≥2510 K and pressures ≥58 GPa in the Earth's interior.⁶



The above-described reaction is favored by the physical catalysis exerted by excited electrons (e^*) that were generated through

stick-sliding during the evolution of supercontinents and mantle conversion triggered by collisions of major asteroids and anti-electron neutrinos $\bar{\nu}_e$ coming from the universe, especially from the young sun from the Archean era to the present time,⁷ or by the radioactive decay of elements such as U and Th and nuclear fusion in the Earth's core that is described later. Equation (1) denotes the endothermic formation of N, O, and water. In contrast to the origin of nitrogen in the Earth, Grewal, Dasgupta, and Marty⁸ inferred that original nitrogen in the Earth is derived from a mixture of both inner and outer solar system materials because the $^{15}\text{N}/^{14}\text{N}$ ratio in the Earth falls between those of the inner and outer solar system. However, their paper cannot explain the reason why a rapid formation of ^{14}N would have continued for 1.3×10^9 years from 2.5 to 3.8×10^9 years ago in the Archean era.⁹

Furthermore, Fukuhara^{10,11} postulated a model for the origin of thermal energy within the Earth's interior, which is devoid of harmful radioactive waste, in which the generated heat is attributed to the three-body nuclear fusion of the deuteron (D) confined within hexagonal FeDx core-center crystals,



The above reaction demonstrates the exothermic formation of the lightest elements H and He. When juxtaposing the conditions for electron degeneracy pressure and temperature for the cores of Jupiter, Saturn, and Earth with those of WISE 1828+2650,¹² the coldest brown dwarf, deuteron nuclear fusion was found to be possible in the cores of Earth, Jupiter, and Saturn, as well as in WISE 1828+2650.¹³

Thus, there is a possibility that Eqs. (1) and (2) show the creation of elements in the Earth's lower mantle or crust and inner core, respectively. Inductively, we considered the possibility of element production from lighter to heavier elements in minerals of the Earth's interior at high pressure and temperature in terms of endothermic nuclear transformable reactions. However, to the best of our knowledge, theories of element creation have not been previously developed in the context of an "Earth factory" as described herein.

II. METHODS

The crystal structures of mineral compounds were drawn by using ATOMS 6.4 (atoms and polyhedra) and CorelDRAW2020 (auxiliary lines and symbols), with the structural data obtained from single-crystal x-ray diffraction measurements¹⁴ for the γ -orthopyroxene ($\text{Mg}_{0.44}\text{Fe}_{0.56}$) SiO_3 mineral, *ab initio* calculations¹⁵ for *Cmcm*- MgAl_2O_4 , and our *ab initio* calculations (VASP 5.3) for the high-pressure kyanite (Al_2SiO_5) III phase.

To calculate the smallest endothermic formation energies, an algorithm was written to iterate through reactant elements and calculate the final values, after which filtering was conducted based on the element type and the final values were obtained. The program provided a total of $\sim 150\,000$ equations, which could then be filtered in a spreadsheet format.

III. RESULTS

A. Comparison of element concentrations of Earth, Mercury, Venus, and Mars

We compare element concentrations of terrestrial planets, namely, Mercury, Venus, Earth, and Mars, which are formed by similar materials. Figure 1(a) shows the variation in the composition of Mercury,¹⁶ Venus,¹⁶ Earth,¹⁶ and Mars¹⁷ for elements with atomic numbers up to 40. The concentrations of Venus, Earth, and Mars elements are roughly similar, unlike Mercury, which is lighter (1/18 of Earth's mass) and hotter (~ 700 K).¹⁶ The concentrations increase to Si and then decrease with the increasing atomic number, regardless of the planet type. Figure 1(b) presents the weight differences of Venus and Mars compared with Earth for elements with atomic numbers from 6 (C) to 26 (Fe), excluding Ne and Ar. The elemental weight differences of Venus and Mars were calculated from their mass ratios relative to that of Earth. The positive values in Fig. 2(b) represent an absolute increase in these elements in Venus and Mars compared with Earth, and negative values indicate a higher ratio on Earth compared to Venus and Mars. The positive values for C and N and the negative values for Cr and Mn in Venus could be derived from the suppression effect, as its atmospheric pressure is ~ 98 -fold

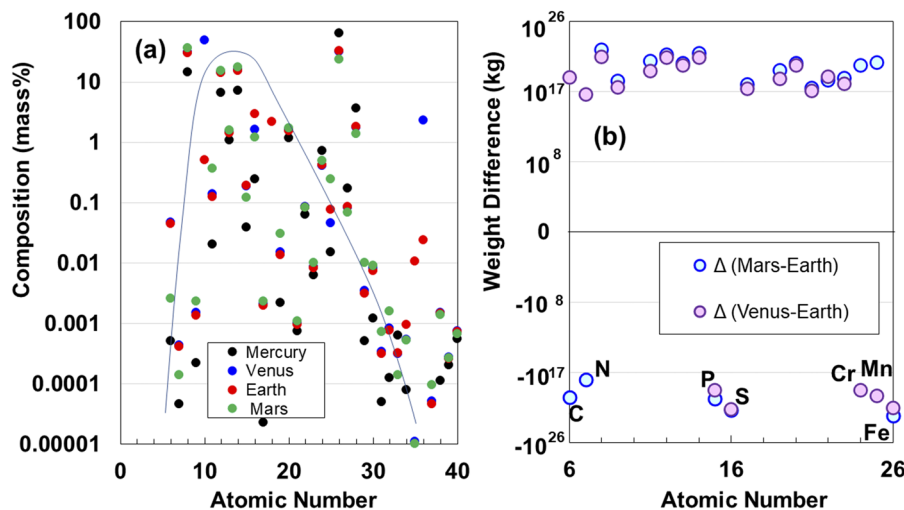


FIG. 1. (a) Atomic number dependent element composition for Mercury, Venus, Earth, and Mars. (b) Weight differences of Venus and Mars to Earth for elements with atomic numbers from 6 to 26.

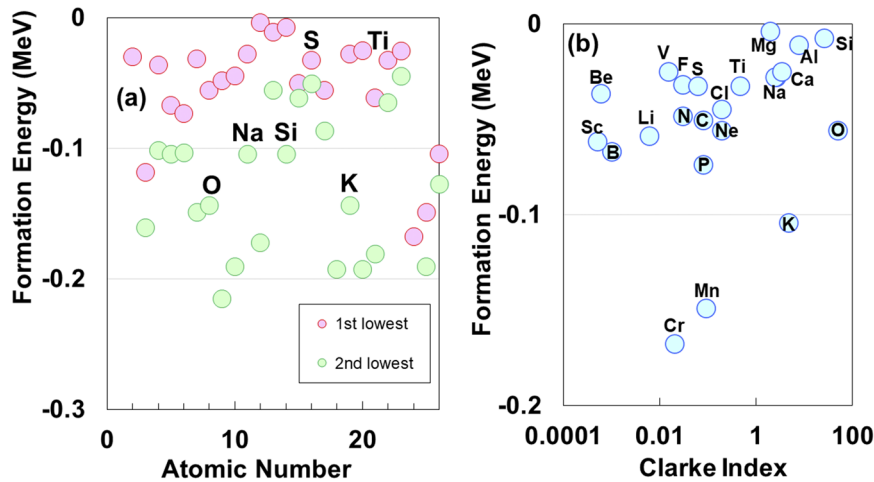


FIG. 2. Formation energies of lighter nuclei up to Ca, as functions of atomic number (a) and Clarke index (b).

higher than that on Earth,¹⁸ and the high vaporization effect of chromium and manganese,¹⁹ respectively. Consequently, C, N, P, S, Cr, Mn, and Fe may have been produced in the Earth's interior after the formation of the terrestrial planets $\sim 4.56 \times 10^9$ years⁴ ago. Even if one considers the collision of asteroids over the past 2.5×10^9 years,²⁰ the sum of all asteroid masses could not exceed over 10^{16} kg. On the other hand, recent research has reported that large amounts of terrestrial N₂,^{21,22} noble gases,²² and O₂²³ have been transported to the Moon via solar wind. This suggests that the atmospheric mass is continuously dispersed into space, and thus, our atmosphere could not keep the pressure needed to support life on Earth without a continuous resupply of these gasses from Earth's interior.

B. Formation of lighter elements in Earth's inside

In Sec. III A, to support the formation of elements in the Earth's internal structure, weight differences of lighter elements of Earth were compared with those of Venus and Mars. Despite the likelihood of the proposed phenomena, it is not possible to secure positive evidence by comparing these data alone.

Therefore, we must consider the endothermic nuclear transmutation for the generation of lighter element nuclei up to ⁵⁶Fe with a mass number of 56 in mineral compounds of Earth's interior. The thermal energy ΔQ for two-body nuclear reactions can be calculated from the rest masses ΔM of the reactants (^AM₁ and ^BM₂) and products (^CM₃, ^DM₄)²⁴ as follows:

$${}^A M_1 + {}^B M_2 = {}^C M_3 + {}^D M_4 + \Delta Q, \quad (3)$$

$$\Delta Q = 931.5 \times \Delta M \text{ (MeV)}, \quad (4)$$

$$\Delta M = ({}^A M_1 + {}^B M_2) - ({}^C M_3 + {}^D M_4), \quad (5)$$

where M is the mass weight²⁵ and A, B, C, and D are mass numbers. In these calculations, we exclude inert gas elements, such as noble gases (e.g., He, Ne, and Ar), and N as reactant nuclei, as they do not appear in natural minerals except for diamond. Due to the irregularities in the atomic number Z and the neutron number N, our result underestimates the nuclear binding energy, which makes

odd nuclei generally less stable. Light elements, such as Li, B, and Mg, have isotopes with lower abundance ratios. Given that nuclear reactions favor light nuclei with smaller radii, we added some light isotopes with a lower abundance ratio in addition to nuclei with higher ones to calculate reaction energies ΔQ . Table I presents the 31 reactant elements with the highest abundance ratio used in this study. The smallest endothermal values ΔQ for each element are given as follows:

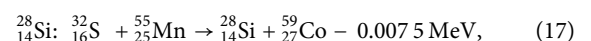
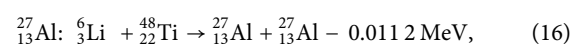
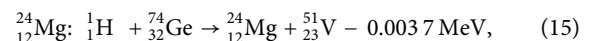
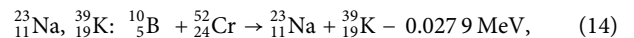
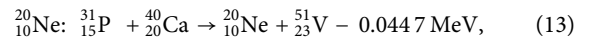
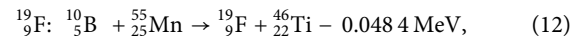
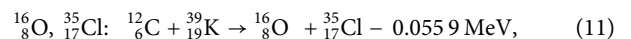
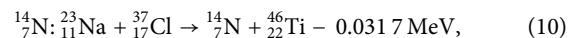
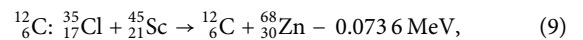
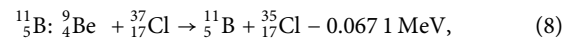
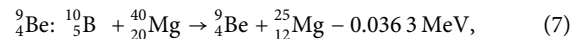
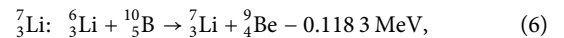


TABLE I. Summary of the 31 reactant element types with the highest abundance ratio used in this study.

${}^6_3\text{Li}$ (7.5)	${}^7_3\text{Li}$ (92.5)	${}^{10}_5\text{B}$ (19.9)	${}^{11}_5\text{B}$ (80.1)	${}^{12}_6\text{C}$ (98.9)	${}^{16}_8\text{O}$ (99.8)	${}^{19}_9\text{F}$ (100)
${}^{23}_{11}\text{Na}$ (100)	${}^{24}_{12}\text{Mg}$ (79.0)	${}^{25}_{12}\text{Mg}$ (10.0)	${}^{26}_{12}\text{Mg}$ (11.0)	${}^{27}_{13}\text{Al}$ (100)	${}^{28}_{14}\text{Si}$ (92.2)	${}^{31}_{15}\text{P}$ (100)
${}^{32}_{16}\text{S}$ (95.0)	${}^{35}_{17}\text{Cl}$ (75.8)	${}^{37}_{17}\text{Cl}$ (24.2)	${}^{39}_{19}\text{K}$ (93.3)	${}^{40}_{20}\text{Ca}$ (96.9)	${}^{48}_{22}\text{Ti}$ (73.8)	${}^{51}_{23}\text{V}$ (99.8)
${}^{52}_{24}\text{Cr}$ (83.8)	${}^{55}_{25}\text{Mn}$ (100)	${}^{56}_{26}\text{Fe}$ (91.7)	${}^{58}_{28}\text{Ni}$ (68.3)	${}^{59}_{27}\text{Co}$ (100)	${}^{60}_{28}\text{Ni}$ (26.1)	${}^{63}_{29}\text{Cu}$ (69.2)
${}^{64}_{30}\text{Zn}$ (48.6)	${}^{66}_{30}\text{Zn}$ (27.9)	${}^{74}_{32}\text{Ge}$ (36.5)				

$${}^{31}_{15}\text{P}: {}^{28}_{14}\text{Si} + {}^{35}_{17}\text{Cl} \rightarrow {}^{31}_{15}\text{P} + {}^{32}_{11}\text{S} - 0.0503 \text{ MeV}, \quad (18)$$

$${}^{32}_{16}\text{S}, {}^{48}_{22}\text{Ti}: {}^{24}_{12}\text{Mg} + {}^{56}_{26}\text{Fe} \rightarrow {}^{32}_{16}\text{S} + {}^{48}_{22}\text{Ti} - 0.0326 \text{ MeV}, \quad (19)$$

$${}^{40}_{20}\text{Ca}, {}^{51}_{23}\text{V}: {}^{28}_{14}\text{Si} + {}^{63}_{29}\text{Cu} \rightarrow {}^{40}_{20}\text{Ca} + {}^{51}_{23}\text{V} - 0.0251 \text{ MeV}, \quad (20)$$

$${}^{45}_{21}\text{Sc}: {}^{37}_{17}\text{Cl} + {}^{39}_{19}\text{K} \rightarrow {}^{31}_{15}\text{P} + {}^{45}_{21}\text{Sc} - 0.0614 \text{ MeV}, \quad (21)$$

$${}^{52}_{24}\text{Cr}: {}^{11}_5\text{B} + {}^{51}_{23}\text{V} \rightarrow {}^{10}_5\text{B} + {}^{52}_{24}\text{Cr} - 0.168 \text{ MeV}, \quad (22)$$

$${}^{55}_{25}\text{Mn}: {}^{24}_{12}\text{Mg} + {}^{45}_{21}\text{Sc} \rightarrow {}^{14}_7\text{N} + {}^{55}_{25}\text{Mn} - 0.1490 \text{ MeV}, \quad (23)$$

$${}^{56}_{26}\text{Fe}: {}^{27}_{13}\text{Al} + {}^{40}_{20}\text{Ca} \rightarrow {}^{11}_5\text{B} + {}^{56}_{26}\text{Fe} - 0.1043 \text{ MeV}. \quad (24)$$

For the second lowest energies, we obtain the following formulas:

$${}^7_3\text{Li}: {}^{23}_{11}\text{Na} + {}^{23}_{11}\text{Na} \rightarrow {}^7_3\text{Li} + {}^{39}_{19}\text{K} - 0.1611 \text{ MeV}, \quad (25)$$

$${}^9_4\text{Be}: {}^7_3\text{Li} + {}^{25}_{12}\text{Mg} \rightarrow {}^9_4\text{Be} + {}^{23}_{11}\text{Na} - 0.1015 \text{ MeV}, \quad (26)$$

$${}^{11}_5\text{B}: {}^{27}_{13}\text{Al} + {}^{40}_{20}\text{Ca} \rightarrow {}^{11}_5\text{B} + {}^{56}_{26}\text{Fe} - 0.1043 \text{ MeV}, \quad (27)$$

$${}^{12}_6\text{C}: {}^{27}_{13}\text{Al} + {}^{48}_{22}\text{Ti} \rightarrow {}^{12}_6\text{C} + {}^{63}_{29}\text{Cu} - 0.1034 \text{ MeV}, \quad (28)$$

$${}^{14}_7\text{N}: {}^{24}_{12}\text{Mg} + {}^{45}_{21}\text{Sc} \rightarrow {}^{14}_7\text{N} + {}^{55}_{25}\text{Mn} - 0.1490 \text{ MeV}, \quad (29)$$

$${}^{16}_8\text{O}, {}^{39}_{19}\text{K}: {}^{27}_{13}\text{Al} + {}^{28}_{14}\text{Si} \rightarrow {}^{16}_8\text{O} + {}^{39}_{19}\text{K} - 0.1434 \text{ MeV}, \quad (30)$$

$${}^{19}_9\text{F}: {}^7_3\text{Li} + {}^{39}_{19}\text{K} \rightarrow {}^{19}_9\text{F} + {}^{27}_{13}\text{Al} - 0.2152 \text{ MeV}, \quad (31)$$

$${}^{20}_{10}\text{Ne}, {}^{55}_{25}\text{Mn}: {}^{23}_{11}\text{Na} + {}^{52}_{24}\text{Cr} \rightarrow {}^{20}_{10}\text{Ne} + {}^{55}_{25}\text{Mn} - 0.1909 \text{ MeV}, \quad (32)$$

$${}^{23}_{11}\text{Na}, {}^{28}_{14}\text{Si}: {}^{24}_{12}\text{Mg} + {}^{27}_{13}\text{Al} \rightarrow {}^{23}_{11}\text{Na} + {}^{28}_{14}\text{Si} - 0.1043 \text{ MeV}, \quad (33)$$

$${}^{24}_{12}\text{Mg}: {}^{16}_8\text{O} + {}^{39}_{19}\text{K} \rightarrow {}^{24}_{12}\text{Mg} + {}^{31}_{15}\text{P} - 0.1723 \text{ MeV}, \quad (34)$$

$${}^{27}_{13}\text{Al}: {}^{24}_{12}\text{Mg} + {}^{66}_{30}\text{Zn} \rightarrow {}^{27}_{13}\text{Al} + {}^{63}_{29}\text{Cu} - 0.0559 \text{ MeV}, \quad (35)$$

$${}^{31}_{15}\text{P}: {}^{37}_{17}\text{Cl} + {}^{39}_{19}\text{K} \rightarrow {}^{31}_{15}\text{P} + {}^{45}_{21}\text{Sc} - 0.0615 \text{ MeV}, \quad (36)$$

$${}^{32}_{16}\text{S}: {}^{28}_{14}\text{Si} + {}^{35}_{17}\text{Cl} \rightarrow {}^{31}_{15}\text{P} + {}^{32}_{16}\text{S} - 0.0503 \text{ MeV}, \quad (37)$$

$${}^{35}_{17}\text{Cl}: {}^{32}_{16}\text{S} + {}^{40}_{20}\text{Ca} \rightarrow {}^{35}_{17}\text{Cl} + {}^{37}_{17}\text{Cl} - 0.0866 \text{ MeV}, \quad (38)$$

$${}^{39}_{19}\text{K}: {}^{27}_{13}\text{Al} + {}^{28}_{14}\text{Si} \rightarrow {}^{16}_8\text{O} + {}^{39}_{19}\text{K} - 0.1434 \text{ MeV}, \quad (39)$$

$${}^{40}_{20}\text{Ca}, {}^{40}_{18}\text{Ar}: {}^{35}_{17}\text{Cl} + {}^{45}_{21}\text{Sc} \rightarrow {}^{40}_{20}\text{Ca} + {}^{40}_{18}\text{Ar} - 0.1928 \text{ MeV}, \quad (40)$$

$${}^{45}_{21}\text{Sc}: {}^{12}_6\text{C} + {}^{65}_{29}\text{Cu} \rightarrow {}^{32}_{16}\text{S} + {}^{45}_{21}\text{Sc} - 0.1807 \text{ MeV}, \quad (41)$$

$${}^{48}_{22}\text{Ti}: {}^{35}_{17}\text{Cl} + {}^{60}_{28}\text{Ni} \rightarrow {}^{47}_{22}\text{Ti} + {}^{48}_{22}\text{Ti} - 0.0652 \text{ MeV}, \quad (42)$$

$${}^{51}_{23}\text{V}: {}^{31}_{15}\text{P} + {}^{40}_{20}\text{Ca} \rightarrow {}^{20}_{10}\text{Ne} + {}^{51}_{23}\text{V} - 0.0447 \text{ MeV}, \quad (43)$$

$${}^{55}_{25}\text{Mn}: {}^{23}_{11}\text{Na} + {}^{52}_{24}\text{Cr} \rightarrow {}^{20}_{10}\text{Ne} + {}^{55}_{25}\text{Mn} - 0.1909 \text{ MeV}, \quad (44)$$

$${}^{56}_{26}\text{Fe}: {}^{26}_{12}\text{Mg} + {}^{55}_{25}\text{Mn} \rightarrow {}^{25}_{12}\text{Mg} + {}^{56}_{26}\text{Fe} - 0.1276 \text{ MeV}. \quad (45)$$

According to the theory of the fundamental process,²⁶ hadronic interaction conserves isospin before and after the endothermic reaction of nuclei.

Given that Eqs. (6)–(45) are non-equilibrium (irreversible) equations, they do not obey the rules of parity and momentum balance. In the irreversible endothermic reaction proposed by Glansdorff and Prigogine,²⁷ remarkable enhancement of formation energy is expected based on the thermal factor of $\exp(-\Delta G/kT)$, where ΔG is the change in Gibbs energy for the whole system. The formation energies with the first and second lowest values are shown in Fig. 2, as functions of atomic number (a) and Clarke index (b), which is the relative abundance of a chemical element in the Earth's crust (i.e., ~1 km below the surface). The lowest energies are below -100 keV, except for Mn. This is especially true for Eqs. (7), (10), (12)–(17), (19), and (20), where Be, N, F, Ne, Na, K, Mg, Al, Si, S, Ti, Ca, and V appear to be formed by endothermic energies below 50 keV. These endothermal energies are approximately close to the acceleration of the $d + d$ reactions in metal lithium acoustic cavitation with deuteron bombardment up to 70 keV.²⁸

If a three-body reaction occurs in place of the above-described two-body reactions, all formation energies in Eqs. (6)–(45) could decrease further.⁷ On the other hand, there is no dependence

between the Clarke number and energy. The Clarke number does not provide the abundance ratio for the entire mass of Earth. Thus, there is a possibility for element creation in the Earth's interior, provided that suitable temperatures and pressures are applied to natural minerals with reactant elements in natural compounds (minerals) of the Earth's interior.

Given that the reactions for Eqs. (6)–(45) are necessary conditions for the nuclear transmutation of lighter elements in Earth's interior, we must investigate sufficient conditions for elements up to iron using minerals at high temperature and pressure. We then considered the potential for nuclear transmutation of natural minerals containing Mg with Fe, Al with Mg, and Al with Si as examples.

C. Transmutation reaction from Mg and Fe

To investigate the endothermic nuclear reaction of $^{32}_{11}\text{S}$ and $^{48}_{22}\text{Ti}$ in natural rocks from Eq. (19), we first selected a stable enstatite-ferrosilite solid solution $[(\text{Mg}, \text{Fe}) \text{SiO}_3]$,²⁹ now known as bridgmanite,³⁰ with a smaller lattice constant at high pressure and high temperature in anticipation of nuclear transmutation between Mg and Fe. The Earth's lower mantle is thought to be composed primarily of aluminous $(\text{Mg}, \text{Fe}) \text{SiO}_3$ perovskite.³¹ Moreover, enstatite (MgSiO_3) and ferrosilite (FeSiO_3) are two crucial endmembers of mantle orthopyroxene. Thus, we chose γ -orthopyroxene ($\text{Mg}_x\text{Fe}_{1-x}\text{SiO}_3$)¹⁴ in its high-pressure form at a temperature exceeding 800 K and pressure above 11.6–21.1 GPa (depending on the ferrosilite content), as a reactant mineral.

Figure 3 illustrates the configuration of the Mg–Fe bond on the (400) plane in the γ -orthopyroxene ($\text{Mg}_{0.44}\text{Fe}_{0.56}$) SiO_3 structure of the high-pressure phase. When γ -orthopyroxene is compressed at a high pressure of 32 GPa, the shortest Mg–Fe distance (d_1) on the (400) plane can be calculated as 0.272 nm. The shrinkage ratio η_1 is 0.9096 ($= 0.272/0.299$). However, the distance d_1 exceeded the distance required for a dynamic nuclear reaction ($\sim 0.094 \text{ nm}$ ³²). Therefore, we must consider the pressure, temperature, and physical catalysis effects accelerating the confinement of magnesium and iron nuclei in the γ -orthopyroxene lattice.

D. Confinement due to high pressure

The outer shell electrons of Mg and Fe atoms in the γ -orthopyroxene ($\text{Mg}, \text{Fe}) \text{SiO}_3$ lattices behave as free electrons,³³ and the resulting screening effect provides relief from the repulsive Coulomb force between Mg and Fe nuclei. The Mg–Fe distance (d_1) of γ -orthopyroxene at 130.3 GPa and 3221 K corresponding 2600 km below the Earth's surface (Sec. 1 in the [supplementary material](#)) can be estimated as 0.1905 nm (see Sec. 2 in the [supplementary material](#)). The shrinkage ratio η_1 is 0.6370 ($= 0.1905/0.299$). However, this distance is still considerable compared to the distance required for a dynamic nuclear reaction.

E. Confinement due to high temperature

Next, we considered the effect of temperature on the reaction rate k . The rate can be expressed using the Arrhenius equation as follows:³⁴

$$k = \frac{k_B T}{h} \frac{f_S f_{\text{Ti}}}{f_{\text{Mg}} f_{\text{Fe}}} e^{-E/RT}, \quad (46)$$

where f_S , f_{Ti} , f_{Mg} , and f_{Fe} are the partition functions of $^{24}_{12}\text{Mg}$, $^{56}_{26}\text{Fe}$, $^{32}_{11}\text{S}$, and $^{48}_{22}\text{Ti}$, respectively, and k_B and R and E are the Boltzmann and gas constants and the activation energy of the reaction, respectively. Because $f_S \approx f_{\text{Ti}} \approx f_{\text{Mg}} \approx f_{\text{Fe}}$, we can express the ratio of the rates at temperatures T_0 and T_1 as follows:

$$\frac{k_1}{k_0} = \frac{T_1}{T_0} e^{\frac{E}{R} \left(\frac{T_1 - T_0}{T_0 T_1} \right)}. \quad (47)$$

If $T_0 = 300 \text{ K}$ and $T_1 = 3221 \text{ K}$, we obtain

$$\frac{k_1}{k_0} \approx 10.737. \quad (48)$$

According to the first principle of the symmetry of force, which is associated with a binding energy, the following potential form expresses the repulsive interaction between atoms:³⁵

$$U(R) = -\frac{B}{r^{12}}, \quad (49)$$

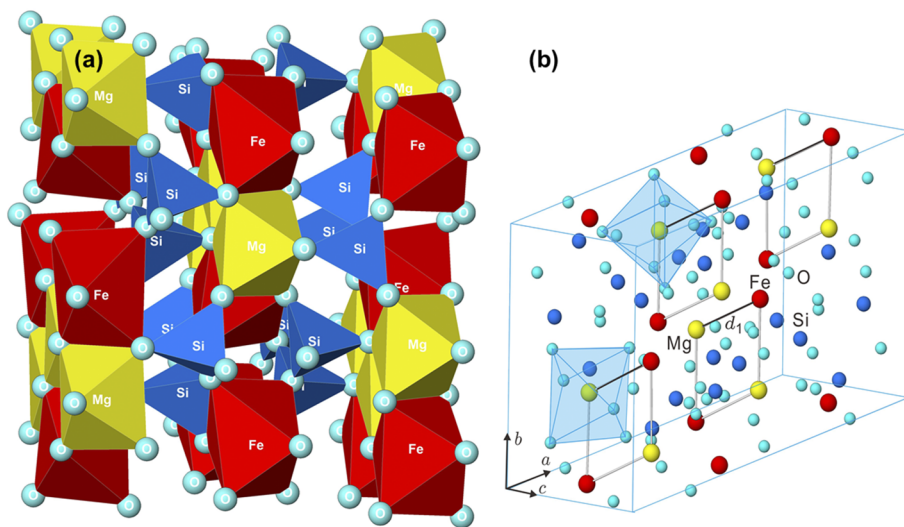


FIG. 3. Structure of γ -orthopyroxene ($\text{Mg}_{0.44}\text{Fe}_{0.56}$) SiO_3 mineral under a high pressure of 32 GPa. (a) Network of oxygen tetrahedra and octahedra. (b) Unit cell, where the shortest Mg–Fe distance is indicated by d_1 .

where B is an empirical parameter. The interaction provides a shrinkage ratio η_2 of 0.8205. Considering the effect of temperature on the reaction rate, we obtained a decreased distance as follows:

$$\begin{aligned} d_2 &\cong 0.8205 \times d_1 = 0.8205 \times 0.6370 \times d_0 \\ &= 0.8205 \times 0.6370 \times 0.299 = 0.1563 \text{ nm}. \end{aligned} \quad (50)$$

However, this radius is approximately double the critical distance (0.094 nm).

F. Effect of physical catalysis on the dynamic reactions between Mg and Fe

The introduction of neutral pions remarkably reduces the inter-nuclear distance between Mg and Fe nuclei, enhancing the fusion rate, which is comparable to physical catalysis³⁶ (Sec. 5 in the [supplementary material](#)). Based on the result of symmetrical meson theory of nuclear force³⁷ and the tendency of energy to clump bosons together, the interaction energy of two nucleons at separation r can be expressed as follows:

$$U(R) = -\frac{A}{r^4}, \quad (51)$$

where A is a coupling constant. Because the addition of two neutral pions increases the attraction force by a factor of 14 when there is a 14-fold increase in the interaction force, we obtain a shrinkage ratio η_3 of 0.5170. The shortest Mg–Fe distance d_3 is calculated using the following formula:

$$\begin{aligned} d_3 &\cong 0.5170 \times d_2 = 0.5170 \times 0.8205 \times d_1 \\ &= 0.5170 \times 0.8205 \times 0.6367 \times 0.299 \\ &= 0.0808 \text{ nm} < \sim 0.094 \text{ nm}^{32}. \end{aligned} \quad (52)$$

This value would promote a nuclear reaction between Mg and Fe nuclei.

Thus, γ -orthopyroxene is a candidate material for nuclear transmutation in the lower mantle.

G. Transmutation reaction involving Al and Mg

Next, we selected MgAl_2O_4 , the main constituent of the mantle, for the endothermic nuclear reaction of $^{23}_{11}\text{Na}$ and $^{28}_{14}\text{Si}$ in natural compounds, as described by Eq. (33). Compounds such as MgAl_2O_4 and Mg_2SiO_4 (olivine) in the mantle are major drivers of plate tectonics and largely determine the physical properties of Earth-type planets.³⁸

MgAl_2O_4 is known to transform from a calcium ferrite (CaFe_2O_4 , CF)-typed structure to a calcium titanate (CaTi_2O_4 , CT)-typed structure at a pressure of ~ 40 GPa.³⁹ An *ab initio* linear combination of atomic orbitals (LCAO) calculation by Catti¹⁵ demonstrated that the calcium titanate structure is more stable compared to the calcium ferrite structure at pressures greater than ~ 39 to 57 GPa.⁴⁰ Thus, we considered nuclear transmutation between Al and Mg nuclei in CT-type MgAl_2O_4 .

Figure 4 presents the structure of *Cmcm*- MgAl_2O_4 under a high pressure of 60 GPa using data obtained from the LCAO calculation.³⁹ Given that the shortest Mg–Al distance (d_1), 0.335 nm, on the (200) plane obtained from Fig. 4 exceeds the distance ($\sim 0.094 \text{ nm}^{32}$) required for a dynamic nuclear reaction, we then accounted for pressure, temperature, and physical catalysis effects accelerating the confinement of magnesium and aluminum nuclei in the *Cmcm*- MgAl_2O_4 lattice. Using shrinkage ratios η_1 (0.7654), η_2 (0.8203), and η_3 (0.5170) for pressure, temperature, and physical catalysis effects, respectively, and provided that *Cmcm*- MgAl_2O_4 exists at 3221 K and 117 GPa corresponding to a depth of 2600 km in the lower mantle region, we obtained the Mg–Al distance d_3 as follows (Sec. 3 in the [supplementary material](#)):

$$\begin{aligned} d_3 &\cong 0.5170 \times d_2 = 0.5170 \times 0.8202 \times d_1 \\ &= 0.5170 \times 0.8202 \times 0.7654 \times 0.2403 \\ &= 0.0780 \text{ nm} < 0.094 \text{ nm}^{32}. \end{aligned} \quad (53)$$

This value would lead to a nuclear reaction between Mg and Al nuclei. The reactant product $^{28}_{14}\text{Si}$ may then be transferred as a constituent element of olivine Mg_2SiO_4 .

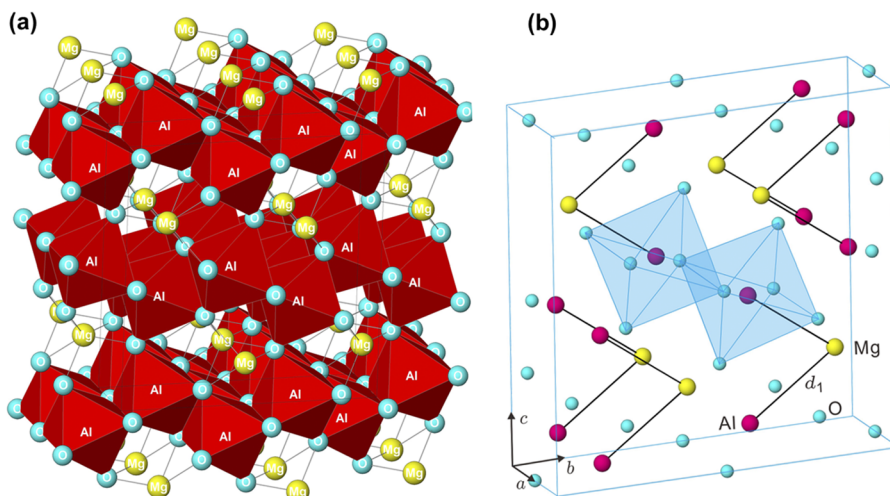


FIG. 4. Structure of *Cmcm*- MgAl_2O_4 under a high pressure of 60 GPa based on data obtained by quantum-mechanical solid-state calculations.¹⁵ (a) Network of oxygen octahedra and interstitial Mg atoms. (b) Unit cell, where the shortest Mg–Al distance is indicated by d_1 .

H. Transmutation reaction involving Al and Si

We then selected a stable aluminosilicate mineral Al_2SiO_5 with a smaller lattice constant at high pressure and high temperature, anticipating the formation of ^{16}O and ^{39}K by endothermic nuclear transmutation between Al and Si in natural compounds, as described in Eq. (30). Al_2SiO_5 is a representative aluminosilicate compound originating from the mantle, which crystallizes near the Earth's surface. It also crystallizes into the three polymorphs, andalusite, sillimanite, and kyanite,⁴⁰ common minerals in metamorphic rocks and important indicators of the pressure and temperature required to form these minerals.⁴¹ Thus, we choose kyanite (Al_2SiO_5) III,⁴⁰ which exists at a high-pressure form at temperatures exceeding 2300 K and pressures above 14 GPa, as a reactant mineral.

Figure 5 illustrates the configuration of the Al–Si–Al chain on the (503) plane in the monoclinic Al_2SiO_5 structure of the high-pressure phase kyanite III. When kyanite is compressed at a high pressure of 23 GPa,⁴² which corresponds to the pressure conditions of the lower-upper mantle boundary, the shortest Al–Si distance (d_1) on the (503) plane can be calculated as 0.2767 nm. However, d_1 exceeds the distance (~ 0.094 nm³²) required for a dynamic nuclear reaction. Therefore, we must consider the pressure, temperature, and physical catalysis effects accelerating the confinement of Al and Si nuclei in the kyanite III lattice. Using the shrinkage ratios η_1 (0.7339), η_2 (0.8203), and η_3 (0.5170) for pressure, temperature, and physical catalysis effects, respectively, and provided that the kyanite III phase exists at 3221 K and 117 GPa, corresponding to a depth of 2600 km in the lower mantle region, we obtained the Mg–Al distance d_3 as follows (Sec. 4 in the [supplementary material](#)):

$$\begin{aligned} d_3 &\cong 0.5170 \times d_2 = 0.5170 \times 0.8203 \times d_1 \\ &= 0.5170 \times 0.8203 \times 0.7339 \times 0.2525 \\ &= 0.0780 \text{ nm} < 0.094 \text{ nm}^{32}. \end{aligned} \quad (54)$$

This value would favor a nuclear reaction between Al and Si nuclei. Kyanite III is a candidate material available for nuclear transmutation in the lower mantle. Andalusite, sillimanite, and kyanite indeed contain some amounts of potassium, which may be indirect evidence for the formation of ^{39}K .

Thus, the formation of lighter elements $^{32}_{11}\text{S}$ and $^{48}_{22}\text{Ti}$, $^{16}_8\text{O}$ and $^{39}_{19}\text{K}$, and $^{23}_{11}\text{Na}$ and $^{28}_{14}\text{Si}$ from natural minerals, such as γ -orthopyroxene (Mg, Fe) SiO_3 , *Cmcm* MgAl_2O_4 , and kyanite III (Al_2SiO_5), respectively, provides a suitable basis for the interpretation of endothermal nuclear reactions. These generated elements immediately react with high-pressure mineral phases of iron magnesium silicates (Mg, Fe) SiO_3 and magnesiowüstites (a combination of magnesium oxide MgO and wüstite FeO), thus forming mixed oxides.

Additionally, we could not select natural compounds containing elements other than Mg, Fe, Al, and Si nor could we identify crystal data relating to pressures over 50 GPa for other minor compound minerals.

I. Geological conditions for the generation of lighter elements

Finally, we considered the geological conditions for the generation of lighter elements. Although the lower mantle could already be present before the formation of the first bona fide continent three billion years ago,²⁰ the generation of large amounts of lighter elements appears to be linked to plate tectonics. The tectonic recycling of ancient materials consisting of granitic magmas has not occurred prior to three billion years ago.⁴³ The mantle convection governing plate tectonics and volcanic activity would have occurred after the nucleation of the liquid core. The nucleation period is thought to have occurred either $3.4\text{--}3.45 \times 10^9$ years ago according to geodynamic measurements⁴⁴ or $2.7\text{--}2.1 \times 10^9$ years ago based on paleomagnetic magnitude research.⁴⁵

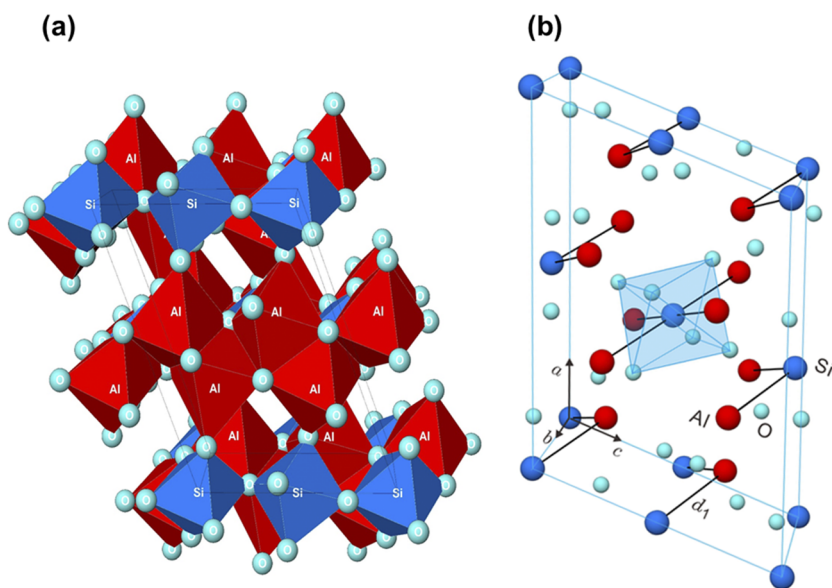


FIG. 5. Structure of the high-pressure phase kyanite (Al_2SiO_5) III at a pressure of 23 GPa. (a) Network of oxygen octahedra. (b) Unit cell, where the shortest Al–Si distance is indicated by d_1 .

Based on the above-described results, the existence of a lower mantle at high temperatures over 3321 K and pressures over 117.3 GPa at a depth of 2600 km could have played a crucial role in the generation of lighter elements. However, the lowest 200 km of the mantle (D'' ; i.e., a region bordering on the core-mantle boundary⁴⁶) is the most chemically heterogeneous active region of the Earth's interior.⁴⁷ In contrast, a suitable region for the generation of lighter elements is likely restricted to locations with a uniform composition and structure up to 2600 km in depth.⁴⁸

The highly active tectonic plate movement coupled with the convection currents of the Earth's mantle (asthenosphere) favors the reactions that mediate the formation of lighter elements. The lithosphere subduction caused by plate tectonics would deliver high quantities of fresh (Mg, Fe) SiO_3 perovskites, MgAl_2O_4 , and aluminosilicate Al_2SiO_5 minerals to the lower mantle, which serve as raw materials for the production of lighter elements. Figure 6 illustrates the process of lighter element formation and discharge by convection currents of the asthenosphere. However, the mantle undergoes slow plastic deformation due to convection speeds of only a few centimeters per year.⁴⁷ Consequently, the upward movement of the resulting compounds occurs over the course of tens to hundreds of millions of years.

As shown in Fig. S5 (supplementary material), asteroid collision events strongly affect the generation of lighter elements⁴¹ due to their important role in continental growth, the

intrusion of granitic magmas, and shifting of the mantle's convection patterns.^{49,50} Studies have reported the occurrence of strong local seismic anisotropy just above the outer core, suggesting the possibility of fluid-dynamical instabilities due to heat from the core trigger plumes of hot rock "jetting" upward toward the surface after tens of millions of years.⁵¹ Nitrogen and helium gases are discharged by volcanic and hydrothermal activities into the atmosphere and are released from the Earth's atmosphere into outer space.

Regarding the physical catalysis attraction mechanism responsible for accelerating the confinement of two nuclei in the natural compound lattices, excited electrons and neutrinos are thought to have been generated by stick sliding^{52,53} during supercontinent evolution,⁵⁴ shifting of the mantle's convection pattern triggered by major asteroid collisions,⁵¹ and nuclear fusion in the Earth's core.¹⁰ The pressure ionization generated under pressures greater than 100 GPa near the Earth's inner core produces excited electrons.^{55,56} Neutrinos are known to be generated by the sun⁵⁷ or in the flares of t-Tauri stars⁵⁸ in the Archean era. Neutrinos are also produced in the Earth's mantle by nuclear fusion in its core^{10,11} or the radioactive decay of elements. Therefore, we propose that there is a very real possibility that nuclear transformation coupled with physical catalysis may have occurred in the Earth's lower mantle. We place our hopes on a future demonstration for the formation of these elements under high temperature and pressure conditions.

The mechanisms proposed in this study were likely influenced by excited electrons generated by stick sliding during the evolution of supercontinents, mantle convection triggered by major asteroid collisions, and nuclear fusion in the Earth's core. The formation of elements heavier than iron will be described in a future paper.

IV. CONCLUSIONS

Our study proposes a potential model for the creation of light element nuclei up to ^{56}Fe with an atomic number of 26 in Earth's interior. The proposed process would result from the endothermal nuclear transmutation of the constituent elements of natural mineral compounds confined by high temperatures and pressures in the lower mantle due to mantle convection dynamics driven by plate tectonics. This study will have a great impact on the geophysical field and as a result will indicate the possible research directions for the potential for the creation of the elements required in future space development.

SUPPLEMENTARY MATERIAL

See the supplementary material for the depth dependence of pressure and temperature in Earth's inside, estimation of the atomic distance between Mg and Fe elements in the γ -orthopyroxene ($\text{Mg}_{0.44}\text{Fe}_{0.56}$) SiO_3 structure at 2650 km below the Earth surface, estimation of the atomic distance between Mg and Al in $\text{Cmcm-MgAl}_2\text{O}_4$ at 2600 km below the Earth surface, estimation of the atomic distance between Al and Si in kyanite III Al_2SiO_5 at 2600 km below the Earth surface, degenerate electrons and pion condensates in the lower mantle region, and asteroid collision-induced atmospheric evolution.

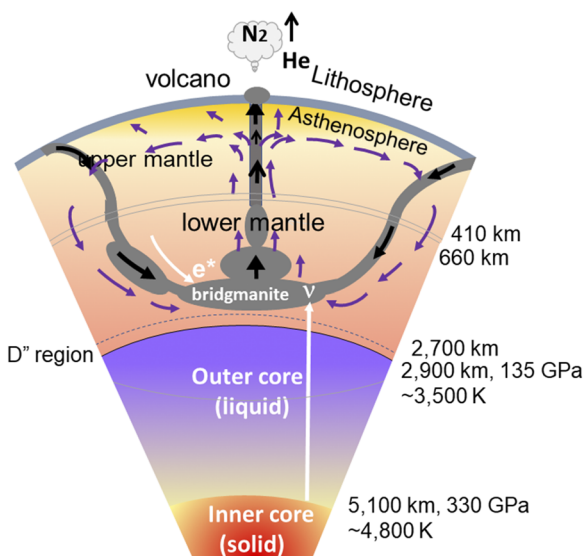


FIG. 6. Cross section of the Earth's interior showing the crust, upper mantle, lower mantle, and outer and inner cores. The formation of lighter elements can be interpreted as the result of endothermic nuclear transmutation of two atom nuclei in natural minerals carried by lithosphere subduction. The process is aided by the physical catalysis of excited electrons (e^*) generated by stick slipping of mineral compounds and geoneutrinos produced deep in the Earth's mantle by nuclear fusion of deuterons and/or radioactive decay of elements.

ACKNOWLEDGMENTS

We would like to acknowledge Editage (www.editage.com) for English language editing.

DATA AVAILABILITY

The data that support the findings of this study are available within the article and its [supplementary material](#) and from the corresponding author upon reasonable request.

REFERENCES

- ¹C. Taylor, "Star factories: Nuclear fusion and the creation of the elements," in *Science in the River City Workshop, 22 March, 2011* (Department of Physics and Astronomy, California State University, 2011).
- ²H. A. Bethe, "Energy production in stars," *Phys. Rev.* **55**, 434–456 (1939).
- ³F. Hoyle, "On nuclear reactions occurring in very hot stars: Synthesis of elements from carbon to nickel," *Astrophys. J.* **1**(Supplement 1), 121–146 (1954).
- ⁴H. E. Newsom and K. W. W. Sims, "Core formation during early accretion of the earth," *Science* **252**, 926–933 (1991).
- ⁵T. Lay, T. J. Ahrens, P. Olson, J. Smyth, and D. Loper, "Studies of the Earth's deep interior: Goals and trends," *Phys. Today* **43**(10), 44–52 (1990).
- ⁶M. Fukuhara, "Did nuclear transformations inside Earth from nitrogen, oxygen, and water?," *J. Phys. Commun.* **4**, 095007 (2020).
- ⁷M. Fukuhara, "Nitrogen discharged from the Earth's interior regions," *J. Mod. Phys.* **5**, 75–81 (2014).
- ⁸D. S. Grewal, R. Dasgupta, and B. Marty, "A very early origin of isotopically distinct nitrogen in inner Solar System protoplanets," *Nat. Astron.* **5**, 356–364 (2021).
- ⁹M. Fukuhara, "Possible origin of nitrogen in the Earth's atmosphere," *Nuovo Cimento C* **27**, 99–113 (2004).
- ¹⁰M. Fukuhara, "Possible generation of heat from nuclear fusion in Earth's inner core," *Sci. Rep.* **6**, 37740 (2016).
- ¹¹M. Fukuhara, "Corrigendum: Possible generation of heat from nuclear fusion in Earth's inner core," *Sci. Rep.* **7**, 46436 (2017).
- ¹²C. Beichman, R. G. Christopher, J. D. Kirkpatrick, T. S. Barman, K. A. Marsh, M. C. Cushing, and E. L. Wright, "The coldest brown dwarf (or free floating planet)?: The Y dwarf WISE 1828+2650," *Astrophys. J.* **764**, 101 (2013).
- ¹³M. Fukuhara, "Possible nuclear fusion of deuterium in the cores of Earth, Jupiter, Saturn, and brown dwarfs," *AIP Adv.* **10**, 035126 (2018).
- ¹⁴J. Xu, D. Fan, D. Zhang, X. Guo, W. Zhou, and P. K. Dera, "Phase transition of enstatite-ferrosilite solid solutions at high pressure and high temperature: Constraints on metastable orthopyroxene in cold subduction," *Geophys. Res. Lett.* **47**, e2020GL087363, <https://doi.org/10.1029/2020GL087363> (2020).
- ¹⁵M. Catti, "High-pressure stability, structure and compressibility of $Cmcm$ - $MgAl_2O_4$: An ab initio study," *Phys. Chem. Miner.* **28**, 729–736 (2001).
- ¹⁶J. W. Morgan and E. Anders, "Chemical composition of Earth, Venus, and Mercury," *Proc. Natl. Acad. Sci. U. S. A.* **77**, 6973–6977 (1980).
- ¹⁷T. Yoshizaki and W. F. McDonough, "The composition of Mars," *Geochim. Cosmochim. Acta* **273**, 137–162 (2020).
- ¹⁸D. R. Williams, Venus Fact Sheet, NASA Goddard Space Flight Center, <http://nssdc.gsfc.nasa.gov/planetary/factsheet/venusfact> 2016.
- ¹⁹Fluid properties: Vapor pressure," in *CRC Handbook of Chemistry and Physics*, 84th ed., edited by R. L. David (CRC Press, Boca Raton, FL, 2003), Sec. 6.
- ²⁰S. Simpson, "Violent origins of continents," *Sci. Am.* **302**, 60–67 (2010).
- ²¹R. Wieler, F. Humbert, and B. Marty, "Evidence for a predominantly non-solar origin of nitrogen in the lunar regolith revealed by single grain analyses," *Earth Planet. Sci. Lett.* **167**, 47–60 (1999).
- ²²M. Ozima, K. Seki, N. Terada, Y. N. Miura, F. A. Podosek, and H. Shinagawa, "Terrestrial nitrogen and noble gases in lunar soils," *Nature* **436**, 655–659 (2005).
- ²³K. Terada, S. Yokota, Y. Saito, N. Kitamura, K. Asamura, and M. N. Nishino, "Biogenic oxygen from Earth transported to the Moon by a wind of magnetospheric ions," *Nat. Astron.* **1**, 0026 (2017).
- ²⁴G. R. Choppin and J. Rydberg, *Nuclear Chemistry: Theory and Applications* (Pergamon Press, New York, 1980), p. 124.
- ²⁵*Physics and Chemistry Dictionary*, 4th ed., edited by R. Kubo, S. Nagakura, H. Iguchi, and H. Ezawa (Iwanami, Tokyo, 1995), pp. 1434–1436.
- ²⁶R. P. Feynmann, *The Theory of Fundamental Processes* (Benjamin-Cummings Publishing Company, San Francisco, CA, 1961), pp. 37, 41.
- ²⁷P. Glansdorff and I. Prigogine, *Thermodynamic Theory of Structure, Stability and Fluctuations* (Wiley-Interscience, London, 1971), p. 1.
- ²⁸Y. Toriyabe, E. Yoshida, J. Kasagi, and M. Fukuhara, "Acceleration of the $d + d$ reaction in metal lithium acoustic cavitation with deuteron bombardment from 30 to 70 keV," *Phys. Rev. C* **85**, 054620 (2012).
- ²⁹H. Yang, R. T. Downs, L. W. Finger, R. M. Hazen, and C. T. Prewitt, "Compressibility and crystal structure of kyanite, Al_2SiO_5 , at high pressure," *Am. Mineral.* **82**, 467–474 (1997).
- ³⁰O. Tschauer, C. Ma, J. R. Beckett, C. Prescher, V. B. Prakapenka, and G. R. Rossman, "Discovery of bridgmanite, the most abundant mineral in Earth, in a shocked meteorite," *Science* **346**, 1100–1102 (2014).
- ³¹A. S. Wolf, J. M. Jackson, P. Dera, and V. B. Prakapenka, *J. Geophys. Res.: Solid Earth* **120**, 7460–7489, <https://doi.org/10.1002/2015jb012108> (2015).
- ³²V. A. Chechin, V. A. Tsarev, M. Rabinowitz, and Y. E. Kim, "Critical review of theoretical models for anomalous effects in deuterated metals," *Int. J. Theor. Phys.* **33**, 617 (1994).
- ³³Ya. B. Zel'dovich and I. D. Novikov, *Relativistic Astrophysics* (Chicago University Press, 1971), Vol. 1, p. 161.
- ³⁴C. Kittel, *Introduction to Solid State Physics*, 6th ed. (John Wiley & Sons, New York, 1986), p. 62.
- ³⁵R. T. Bush and R. D. Egleton, "'Cold nuclear fusion': A hypothetical model to probe on elusive phenomenon," *J. Fusion Energy* **9**, 397–408 (1990).
- ³⁶M. Fukuhara, "Neutral pion-catalyzed fusion in palladium lattice," *Fusion Sci. Technol.* **43**, 128–133 (2003).
- ³⁷D. F. Measday and G. A. Miller, "Hopes and realities for the (p, π) reaction," *Annu. Rev. Nucl. Part. Sci.* **29**, 121–160 (1983).
- ³⁸A. Yoshiasa, H. Maekawa, and K. Sugiyama, "Crystal chemistry of $MgAl_2O_4$ spinel solid solution-peculiar presence of cation observed under substitution and pressure," *J. Crystallogr. Soc. Jpn.* **53**, 13–18 (2011).
- ³⁹N. Funamori, R. Jeanloz, J. H. Nguyen, A. Kavner, W. A. Caldwell *et al.*, "High-pressure transformations in $MgAl_2O_4$," *J. Geophys. Res.* **103**, 20813–20818, <https://doi.org/10.1029/98jb01575> (1998).
- ⁴⁰T. Irifune and T. Tsuchiya, "2.03 mineralogy of the earth-phase transitions and mineralogy of the lower mantle," in *Treatise on Geophysics*, edited by G. Schubert (Elsevier, Oxford, 2015), pp. 33–61.
- ⁴¹M. Arima, Y. Oka, and Y. Hariya, "Stability relationship between sillimanite solid solution and kyanite in the system Al_2O_3 - SiO_2 at high pressures and temperatures," *J. Mineral. Petrol. Eco. Geol. Spec.* **1**, 143–151 (1976) [in Japanese].
- ⁴²Y. Zhou, T. Irifune, H. Ohfuji, and T. Kuribayashi, "New high-pressure forms of Al_2SiO_5 ," *Geophys. Res. Lett.* **45**, 8167–8172, <https://doi.org/10.1029/2018gl078960> (2018).
- ⁴³R. S. Taylor and S. M. McLennan, "The evolution of continental crust," *Sci. Am.* **274**, 60–65 (1996).
- ⁴⁴J. A. Tarduno *et al.*, "Geodynamo, solar wind, and magnetopause 3.4 to 3.45 billion years ago," *Science* **327**, 1238–1240 (2010).
- ⁴⁵C. J. Hale, "Palaeomagnetic data suggest link between the Archaean-Proterozoic boundary and inner-core nucleation," *Nature* **329**, 233–237 (1987).
- ⁴⁶K. Bullen, "Compressibility-pressure hypothesis and the Earth's interior," *Mon. Not. R. Astron. Soc.* **5**, 355–368 (1949).
- ⁴⁷R. Jeanloz and B. Romanowicz, "Geophysical dynamics at the center of the Earth," *Phys. Today* **50**(8), 22–27 (1997).
- ⁴⁸T. Lay, Q. Williams, and E. J. Garnero, "The core-mantle boundary layer and deep Earth dynamics," *Nature* **392**, 461–468 (1998).
- ⁴⁹R. Jeanloz and T. Lay, "The core-mantle boundary," *Sci. Am.* **268**, 48 (1993).
- ⁵⁰R. A. F. Grieve, "Impact bombardment and its role in proto-continental growth on the early Earth," *Precambrian Res.* **10**, 217–247 (1980).

- ⁵¹A. Glikson, "Field evidence of Eros-scale asteroids and impact forcing of Precambrian geodynamic episodes, Kaapvaal (South Africa) and Pilbara (Western Australia) cratons," *Earth Planet. Sci. Lett.* **267**, 558–570 (2008).
- ⁵²J. N. Brune, S. Brown, and P. A. Johnson, "Rupture mechanism and interface separation in foam rubber models of earthquakes: A possible solution to the heat flow paradox and the paradox of large overthrusts," *Tectonophysics* **218**, 59–67 (1993).
- ⁵³A. Tsutsumi and N. Shirai, "Electromagnetic signals associated with stick-slip of quartz-free rocks," *Tectonophysics* **450**, 79–84 (2008).
- ⁵⁴D. Bercovici, "Mantle convection," in *Encyclopedia of Solid Earth Geophysics*, edited by H. Gupta (Springer, The Netherlands, 2011), pp. 832–851.
- ⁵⁵D. S. Kothari, "The theory of pressure-ionization and its applications," *Proc. R. Soc. London, Ser. A* **165**, 486–500 (1938).
- ⁵⁶A. I. Pisarenko and A. A. Yatsenko, "Pressure ionization of hydrogen and helium," *Astron. Rep.* **52**, 937–940 (2008).
- ⁵⁷L.-A. McFadden and T. V. Johnson, *Encyclopedia of the Solar System*, edited by P. R. Weissman, L.-A. McFadden, and T. V. Johnson (Academic Press, San Diego, 1999), p. 68.
- ⁵⁸A. Unsöld, *Der Neue Kosmos*, 2nd ed. (Springer-Verlag, Berlin, 1974), p. 226.